The Scientific Temper (2024) Vol. 15 (3): 2460-2464
E-ISSN: 2231-6396, ISSN: 0976-8653
Doi: 10.58414/SCIENTIFICTEMPER.2024.15.3.07
https://scientifictemper.com/

RESEARCH ARTICLE

Amelioration of the UV-blocking property of ZnO nanoparticles as an active sunscreen ingredient

Sampa Mondal[1], Baibaswata Bhattacharjee[2*]

Abstract

ZnO nanoparticles are synthesized employing simple wet chemical methods and different samples are prepared by varying liquid mediums (consecutively water medium, ethanol medium, methanol medium) in the initial solution to tailor the ultraviolet (UV) ray blocking proficiency. All samples are evaluated for optical, microstructural, and compositional characteristics. The line shape of UV-vis spectra of ZnO nanoparticles shows interesting and remarkable changes with varying synthesis conditions. The fascinating observation of generating high %UVA-blocking and %UVB-blocking can be attributed to getting control over the UV-vis spectra of synthesized ZnO nanoparticles. These NPs can provide full protection from total UVA and UVB regions due to their high %UVA-blocking and %UVB-blocking values. When the experimental settings are changed (from water medium to ethanol medium then to methanol), the %UVA-blocking and %UVB-blocking is highest for the sample synthesized in methanol medium, lower for the sample synthesized in ethanol medium and lowest for the sample synthesized in water medium. However, compared with some popular commercial sunscreen brands, the photoprotection ability of all ZnO nanoparticles is higher than that of the popular sunscreen products. The facile technique adopted in this work opens up an easy way to synthesize ZnO nanoparticles (NPs) with a broad absorption spectrum in the UV area which can provide full protection from the whole UVA and UVB ranges.

Keywords: ZnO nanoparticles, UV absorption, Sunscreen, %UVA-blocking, %UVB-blocking.

Introduction

Human skin exposed to ultraviolet radiation (UVR) suffers negative effects (Zhang *et al.*, 2024). The need for UV light protection is, therefore, essential (Berry *et al.*, 2022). Three kinds of UVR are emitted by the sun: UVA (320–400 nm), UVB (290–320 nm), and UVC (200–290 nm) (Geoffrey *et al.*, 2019). Among these radiations, the most harmful form is UVC (200–290 nm), which is suppressed by the ozone layer of the atmosphere before it reaches the earth's surface. 5 %UVB and 95 %UVA radiation from the sun's UV spectrum reach the earth's surface (Tang *et al.*, 2024).

Sunscreens are employed to shield the skin from the harmful effects of UVR from the sun by preventing and reducing these effects (Chen *et al.*, 2023). Based on the method of administration, sunscreen ingredients are generally divided into systemic and topical categories. Topical sunscreen agents are further classified into two kinds based on their mechanism of protection: organic (also known as chemical) and inorganic (commonly known as mineral) compounds (Rajasekar *et al.*, 2024). On the other hand, they are generally divided into three types based on the range of protection: UVB (290–320 nm) and UVA (320–400 nm), as well as board spectrum sunscreen agents that cover the entire spectrum (290–400 nm). Systemic sunscreen ingredients are absorbed by the body and build up on the skin, protecting against UVR (Lee *et al.*, 2024). Systemic sunscreen agents include aspirin, ascorbic acid, retinol, selenium, and others. Since topical sunscreens predominate on the market and systemic sunscreens are rarely used in daily routine, topical sunscreens are the focus of this article. High-energy UVR is absorbed by organic sunscreen ingredients (B. L. Diffey *et al.*, 2000). Examples of organic sunscreen agents are salicylates, octocrylene, avobenzone, cinnamates, etc. Inorganic sunscreen ingredients are substances that

[1]Department of Physics, Bankura Zilla Saradamani Mahila Mahavidyapith, Bankura, West Bengal, India.

[2]Department of Physics, Ramananda College, Bankura, West Bengal, India.

***Corresponding Author:** Baibaswata Bhattacharjee, Department of Physics, Ramananda College, Bankura, West Bengal, India, E-Mail: baib23@gmail.com

How to cite this article: Mondal, S., Bhattacharjee, B. (2024). Amelioration of the UV-blocking property of ZnO nanoparticles as an active sunscreen ingredient. The Scientific Temper, **15**(3):2460-2464.
Doi: 10.58414/SCIENTIFICTEMPER.2024.15.3.07

Source of support: Nil

Conflict of interest: None.

Received: 09/07/2024 **Accepted:** 17/08/2024 **Published** : 10/09/2024

disperse and reflect UVR into the surrounding space (Lee *et al*., 2024). They serve as a physical deterrent to ultraviolet and indent light. Titanium dioxide NPs and zinc oxide NPs are the two most widely utilized inorganic sunscreen agents (V. Samuthira Pandi *et al*., 2023). Sunblocks are another name for inorganic sunscreens. There are various sunscreen products on the market, but it is still unsure whether or not they are effective or safe. So, it is important to increase the UV-blocking properties of sunscreen ingredients (B. Diffey, 2001; Gasparro *et al*., 1998).

It has become possible to synthesize ZnO nanoparticles (NPs) that have a broad absorption spectrum throughout the UVA and UVB region and that can provide full protection from the whole UVA and UVB region. As a result, one of the most significant uses of ZnO NPs in biomedical applications is as sunscreen agents because of their distinctive optical characteristics. The primary objective of this study is to enhance the UV-blocking ability of ZnO NPs, which can be efficiently used as the active ingredient of ZnO-based sunscreens because of their distinctive optical characteristics.

Materials and Methods

Materials

Zinc chloride (Sigma-Aldrich, purity 99.99%), sodium hydroxide (Sigma-Aldrich, purity 99.99%), distilled deionized (DI) water (Merck, purity 99.99%), ethanol, and methanol are utilized as bought.

Synthesis of ZnO NPs

The co-precipitation approach, which involves the controlled precipitation of NPs from the solution of precursors, is used to synthesize ZnO NPs. Various liquid mediums have been used in different synthesis methods to enhance the UV-blocking properties of ZnO NPs. ZnO NPs are synthesized using a simple wet chemical method and other samples are synthesized with varying liquid medium in the starting solution as shown in Table 1. Under continual stirring at 60°C, 0.011 mol of zinc chloride ($ZnCl_2$) and 0.125 mol of sodium hydroxide (NaOH) are dissolved in 200 and 150 mL of a liquid medium as shown in Table 1, respectively. NaOH solution is then dropped into the $ZnCl_2$ solution, and the resulting milky white solution with no precipitation is stirred for 45 minutes at 60°C. The solution is filtered and dried outside in the open air after being washed five times with DI water. ZnO NPs can be produced as a white powder.

Table 1: Design of experiment for the formation of ZnO NPs and sample name of different ZnO NPs according to the experimental conditions

Liquid medium	*Sample name*
Water	ZnO – 1
Ethanol	ZnO – 2
Methanol	ZnO – 3

%UVA-blocking and %UVB-blocking Value Measurement

For photoprotection studies, a sample of commercial sunscreen weighing 0.02 g is put into a volumetric flask measuring 100 mL. About 70 mL of 70% isopropyl alcohol is added into the volumetric flask. The solution is firmly shaken and then diluted to the mark with the 70% isopropyl alcohol. Each sunscreen product undergoes three trials, with each solution's absorbance measured from 250 to 1000 nm using a UV-vis spectrophotometer. The following formula is used to determine the adjusted absorbance (A) (Chou *et al*., 2017):

$$A = Measured\ A \times \frac{mass\ of\ sunscreen\ ingredient}{mass\ of\ solution} \quad (1)$$

For precision and consistency, the mean corrected absorbance of the three readings is determined. In the case of ZnO NPs, 0.005 g of samples are taken and the next step is identical to that mentioned above. Equation 1 is used to determine the adjusted absorbance.

Characterizations and Instrumentations

Using a Bruker D8 Advance diffractometer, the crystallinity of the ZnO NPs is assessed throughout an angular range (2θ) of 20 to 80°. A Zeiss Sigma field-enhanced secondary electron microscope (FESEM) is used to examine the morphology of the produced ZnO NPs. A Jasco V-770 spectrophotometer is used to record UV-vis absorption spectra spanning the wavelength range of 250 to 1000 nm.

Results and Discussion

X-ray diffraction

The X-ray diffraction (XRD) spectra of ZnO-1 are shown in Figure 1 as a representative. The nature of the peaks is found to be broad, depicting the nanoparticle nature of the sample. The sample exhibits common peaks located at 2θ positions of 31.84°, 34.45°, 36.28°, 47.55°, 56.64°, 62.84°, 66.47°, 67.96°, 69.20°, 72.64°, 76.94° which are attributed to the crystal planes 100, 002, 101, 012, 110, 013, 200, 112, 201, 004, 011, respectively, where ZnO NPs has a hexagonal crystal structure (Gherbi *et al*., 2022). The other samples also exhibit the diffraction peaks at almost the same 2θ values, confirming no phase alteration in the samples despite a change in the reaction medium during the synthesis.

The mean size of the NPs is determined using the Debye-Sherrer formula and the following equation (Bhattacharyya *et al*., 2011; Da Silva *et al*., 2024; He *et al*., 2023; Kumar *et al*., 2023):

$$D = \frac{0.89\ \lambda}{\beta\ cos\theta} \quad (2)$$

Where λ is the wavelength of the X-ray used (here λ = 1.54 Aº for Cu K_α radiation), θ is the Bragg angle, the full width at half maximum (FWHM) of the X-ray diffraction peak is β and the shape factor is 0.89. The mean particle sizes of ZnO NP samples are given in Table 2.

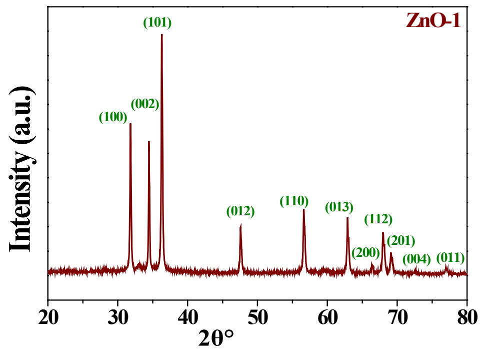

Figure 1: XRD patterns of ZnO-1

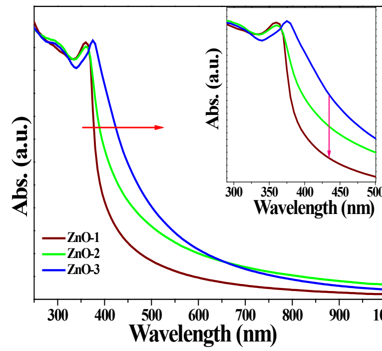

Figure 3: UV-vis absorption spectrum of ZnO-1, ZnO-2, and ZnO-3

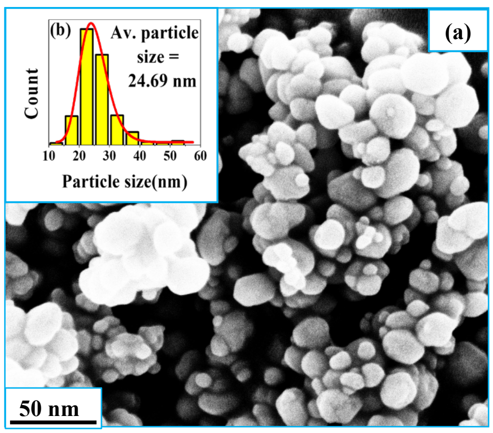

Figure 2: (a) FESEM images of ZnO-1, (b) Particle size distribution histograms of ZnO-1

Table 2: Estimated particle size from XRD and SEM, and energy band gap of ZnO. NPs obtained under different experimental conditions

Sample name	*Average particle size (nm) from XRD*	*Average particle size (nm) from SEM*	*Band gap energy (eV)*
ZnO - 1	23.90	24.69	3.22
ZnO - 2	25.90	25.50	3.05
ZnO - 3	27.59	27.48	2.98

Morphological Investigation

The particle size and particle size distribution of ZnO NPs are investigated using the FESEM micrographs. The FESEM image of ZnO-1 is displayed in Figure 2a as a representative. The shape of the majority of ZnO NPs is found to be spherical or spheroidal. Figure 2b shows the particle size distribution histogram that is obtained from this FESEM image along with the theoretical curve fitted with the particle size distribution data. The particle size is found to follow the log-normal distribution pattern, which is common for samples containing very small particles. The other two samples also exhibit spherical or spheroidal particles and follow the same type of particle distribution pattern. The average particle sizes estimated through morphological investigation are displayed in Table 2.

UV-VIS spectroscopy

The broad absorption spectra throughout the UVA and UVB regions of the produced ZnO NPs for different synthesis methods are shown in Figure 3. Significant variation in the line shape of absorption spectra beyond the absorption edge is observed with changing the liquid mediums (Table 1) in the initial solution (Figure 3, inset). When the experimental settings are changed (consecutively water medium, ethanol medium, and methanol medium), the steepness of absorption spectra is greatest for ZnO-1, lower for ZnO-2, and lowest for ZnO-3. However, the absorption spectra of all samples cover the total UVA and UVB region (Figure 3). The optical bandgaps of the as-prepared ZnO NPs are estimated using the Tauc plot by plotting $(\alpha h\nu)^2$ against hν and extrapolating the band edge slope against zero (Morales-Mendoza *et al.*, 2021; Parimala & Ganeshkumar, 2024; Velumani *et al.*, 2024; Yasmin *et al.*, 2021). The estimated optical bandgaps of NPs are given in Table 2. According to Table 2, the lower band gap value of ZnO NPs compared to bulk materials (3.3 eV) can be attributed to planar defect.

Figure 4 shows the absorption spectra of 3 different popular sunscreen products. However, the absorption spectra of brand-A do not cover the total UVA region (Figure 4a), which means it cannot protect from total UVA rays. On the other hand, brand B does not have broad absorption spectra throughout the UVA and UVB regions (Figure 4b). In addition, the absorption spectra of brand-C cover total UVA and UVB regions, but the steepness of the absorption spectra is extremely low (Figure 4c). However, the UVA and UVB blocking ability of all NPs is better than that of popular

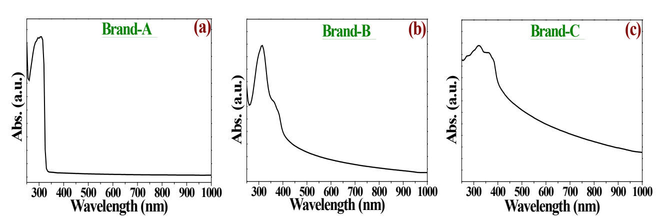

Figure 4: UV-vis absorption spectrum of brand-A, Brand-B, and Brand-C

sunscreen products because of their broad absorption spectra throughout the UVA and UVB regions.

%UVA-blocking and %UVB-blocking Studies

The effectiveness of sunscreen agents mainly depends on photoprotection. Photoprotection refers to the ability of the sunscreen ingredients to protect against UVA and UVB rays. However, the factors that define a sun-blocking agent's efficacy and effectiveness include the %UVA-blocking and %UVB-blocking.

%UVA-blocking

The %UVA-blocking indicates the percentage of UVA rays blocked by sun screening agents. The following equations can be used to determine the %UVA-blocking of sun screening ingredients (Berry *et al*., 2022):

$$T(UVA) = \frac{\int_{320}^{400} T_\lambda \, d\lambda}{\int_{320}^{400} d\lambda} \tag{3}$$

Where T_λ is the diffuse transmittance spectrum (%). This information is frequently presented as %UVA blocking = 100% - T (UVA), where T (UVA) is a percentage (Berry *et al*., 2022). The calculated %UVA-blocking of all samples is given in Table 3.

%UVB-blocking

The %UVB-blocking shows the percentage of UVB radiation that can be blocked by sunscreen agents. The equations shown below can be used to calculate %UVB-blocking (Berry *et al*., 2022):

$$T(UVB) = \frac{\int_{290}^{320} T_\lambda \, d\lambda}{\int_{290}^{320} d\lambda} \tag{4}$$

Where T_λ is the diffuse transmittance spectrum (%). The formula for these values is frequently given as %UVB blocking = 100% - T (UVB), where T (UVB) is a percentage (Berry *et al*., 2022). The estimated %UVB-blocking is displayed in Table 3.

Evaluation of the %UVA-blocking and %UVB-blocking value

The %UVA-blocking and %UVB-blocking values are calculated by using Equation 3 and 4, respectively. The values of %UVA-blocking and %UVB-blocking of all NPs and three popular commercial sunscreen products are given in Table 3.

According to Table 3, brand-A is unable to protect against UVA rays, as seen by its high %UVB-blocking value, and extremely low %UVA-blocking value. Table 3 shows that while brand-B has a moderate %UVB-blocking value and a low %UVA-blocking value, indicating it is incapable of offering high photoprotection against the total UVB and UVA region. On the other hand, brand-C has moderate %UVA-blocking and %UVB-blocking values, which means it cannot provide high photoprotection from total UVA and UVB regions.

The results shown in Table 3 demonstrate that all of the synthesized NPs have high %UVA-blocking and %UVB-blocking values, confirming that they are capable of providing high photoprotection against the total UVA and UVB rays. Additionally, only brand-C of the commercial brands has a moderate value of %UVB-blocking and %UVA-blocking; however, ZnO NPs synthesized under different experimental conditions have greater %UVA-blocking and %UVB-blocking values than brand-C. Furthermore, each nanoparticle has greater %UVA-blocking and %UVB-blocking values than other well-known brands, proving the remarkable photoprotection efficiency of these NPs.

Table 3: The calculated value of %UVA-blocking and %UVB-blocking of three different sunscreen products and all ZnO NPs

Sample	*%UVA -blocking*	*%UVB-blocking*
Brand-A	25.37	99.65
Brand-B	76.39	90.62
Brand-C	91.40	92.84
ZnO-1	98.01	99.54
ZnO-2	99.38	99.81
ZnO-3	99.74	99.82

So, using these synthesis methods the UV-blocking property of ZnO NPs is tailored. As shown in Table 3, %UVA-blocking and %UVB-blocking values rise with changing the liquid medium in the starting solution, according to Table 1. When the experimental settings are changed (Table 1), the %UVA-blocking and %UVB-blocking are highest for ZnO-3, lower for ZnO-2, and lowest for ZnO-1. So, compared to other ZnO NPs, ZnO-3 has more photoprotective ability. However, all NPs can be considered as broad-spectrum sunscreen agents with outstanding photoprotection due to their high %UVA-blocking and %UVB-blocking values. In addition, the photoprotection ability of all NPs is better than that of popular sunscreen products.

Conclusion

A simple and low-cost wet chemical method has been used to produce high-grade, pure, highly crystalline wurtzite-structured ZnO NPs with varying liquid mediums in the starting solution during synthesis. SEM and XRD investigations confirm that excellent ZnO nanoparticles are produced. The %UVA-blocking and %UVB-blocking values of each NPs are very high. The advanced photoprotective capability of all ZnO NPs results in greater effectiveness than in several well-known commercial brands. Compared with the different ZnO samples, ZnO-3 has the greatest %UVA-blocking and %UVB-blocking values than the other two samples. However, ZnO-3 exhibits greater effectiveness as a sunscreen ingredient than other ZnO NPs. As a result of their unique optical properties, one of the most important uses of ZnO NPs in the biomedical arena is as sunscreen agents. The simple approach used in this study makes it possible to easily produce ZnO NPs with amazing photoprotection efficiency due to their high %UVA-blocking and %UVB-blocking values. Thus, our study also offers a simple and easy way to regulate the UVA-blocking and %UVB-blocking values of ZnO NPs. These ZnO NPs can be efficiently used as the active ingredient of ZnO-based sunscreens.

Acknowledgment

The authors would like to acknowledge the Co-ordinator, Centre of Excellence in Advanced Materials, National Institute of Technology Durgapur, for microstructural characterization.

References

Berry, E. G., Bezecny, J., Acton, M., Sulmonetti, T. P., Anderson, D. M., Beckham, H. W., Durr, R. A., Chiba, T., Beem, J., Brash, D. E., Kulkarni, R., Cassidy, P. B., & Leachman, S. A. (2022). Slip versus Slop: A Head-to-Head Comparison of UV-Protective Clothing to Sunscreen. *Cancers*, *14*(3), 542. https://doi.org/10.3390/cancers14030542

Bhattacharyya, A., Datta, P. S., Bhaumik, A., Viraktamath, S., Chowdhury, M. U., & Isaac, R. K. (2011). TINY DEVICES-NANO - THE EMERGING WORLD TECHNOLOGY. *The Scientific Temper*, *2*(1 & 2), 9–14. https://doi.org/10.58414/SCIENTIFICTEMPER.2011.02.1.02

Chen, M., Hua, J., & Jiang, Q. (2023). Preparation and Performance Study of ZnO Nanorod Array with Anti-Ultraviolet and Superhydrophobic Surface. *Nano*, *18*(09), 2350070. https://doi.org/10.1142/S1793292023500704

Chou, J., Robinson, T. J., & Doan, H. (2017). Rapid Comparison of UVB Absorption Effectiveness of Various Sunscreens by UV-Vis Spectroscopy. *Journal of Analytical & Bioanalytical Techniques*, *08*(02). https://doi.org/10.4172/2155-9872.1000355

Da Silva, M. R. P., Matos, R. S., Monteiro, M. D. S., Da Fonseca Filho, H. D., Ramos, G. Q., Santos, S. B., Andrade, G. S., Andrade, G. R. S., & Almeida, L. E. (2024). Defect-engineered Ag/ZnO and Ag2O/ZnO nanomaterials prepared with nanoparticles synthesized by a sustainable sol–gel method and their biological responses. *Journal of Nanoparticle Research*, *26*(4), 69. https://doi.org/10.1007/s11051-024-05973-w

Diffey, B. (2001). Sunscreen isn't enough. *Journal of Photochemistry and Photobiology B: Biology*, *64*(2–3), 105–108. https://doi.org/10.1016/S1011-1344(01)00195-6

Diffey, B. L., Tanner, P. R., Matts, P. J., & Nash, J. F. (2000). In vitro assessment of the broad-spectrum ultraviolet protection of sunscreen products. *Journal of the American Academy of Dermatology*, *43*(6), 1024–1035. https://doi.org/10.1067/mjd.2000.109291

Gasparro, F. P., Mitchnick, M., & Nash, J. F. (1998). A Review of Sunscreen Safety and Efficacy. *Photochemistry and Photobiology*, *68*(3), 243–256. https://doi.org/10.1111/j.1751-1097.1998.tb09677.x

Geoffrey, K., Mwangi, A. N., & Maru, S. M. (2019). Sunscreen products: Rationale for use, formulation development and regulatory considerations. *Saudi Pharmaceutical Journal*, *27*(7), 1009–1018. https://doi.org/10.1016/j.jsps.2019.08.003

Gherbi, B., Laouini, S. E., Meneceur, S., Bouafia, A., Hemmami, H., Tedjani, M. L., Thiripuranathar, G., Barhoum, A., & Menaa, F. (2022). Effect of pH Value on the Bandgap Energy and Particles Size for Biosynthesis of ZnO Nanoparticles: Efficiency for Photocatalytic Adsorption of Methyl Orange. *Sustainability*, *14*(18), 11300. https://doi.org/10.3390/su141811300

He, Z., Zhang, W., Xie, X., Guo, J., Zhang, X., & Wang, J. (2023). Preparation and photoelectrochemical properties of TiO2/ZnO nanorod heterojunction arrays. *Journal of Nanoparticle Research*, *25*(11), 226. https://doi.org/10.1007/s11051-023-05878-0

Kumar, N., Vikram Delu, Tarsem Nain, Anil Kumar, Pooja, & Arbind Acharya. (2023). Exploring the therapeutic implications of nanoparticles for liquid tumors: A comprehensive review with special emphasis on green synthesis techniques in the context of Dalton's lymphoma. *The Scientific Temper*, *14*(03), 916–926. https://doi.org/10.58414/SCIENTIFICTEMPER.2023.14.3.55

Lee, S. J., Lee, D., Park, S. A., Park, J. J., & Park, W. H. (2024). Hyaluronic acid/polyphenol sunscreens with broad-spectrum UV protection properties from tannic acid and quercetin. *International Journal of Biological Macromolecules*, *257*, 128585. https://doi.org/10.1016/j.ijbiomac.2023.128585

Morales-Mendoza, J. E., Herrera-Pérez, G., López-Martinez, E. I., Lardizabal-Gutierrez, D., & Paraguay-Delgado, F. (2021). Microstructural and optical properties of ZnO coatings from colloidal inks. *Journal of Nanoparticle Research*, *23*(2), 34. https://doi.org/10.1007/s11051-021-05153-0

Parimala, V., & Ganeshkumar, D. (2024). Solar energy-driven water distillation with nanoparticle integration for enhanced efficiency, sustainability, and potable water production in arid regions. *The Scientific Temper*, *15*(01), 1644–1651. https://doi.org/10.58414/SCIENTIFICTEMPER.2024.15.1.11

Rajasekar, M., Mary, J., Sivakumar, M., & Selvam, M. (2024). Recent developments in sunscreens based on chromophore compounds and nanoparticles. *RSC Advances*, *14*(4), 2529–2563. https://doi.org/10.1039/D3RA08178H

Tang, X., Yang, T., Yu, D., Xiong, H., & Zhang, S. (2024). Current insights and future perspectives of ultraviolet radiation (UV) exposure: Friends and foes to the skin and beyond the skin. *Environment International*, *185*, 108535. https://doi.org/10.1016/j.envint.2024.108535

Velumani, M., Rajamohan, S., Pandey, A., Pham, N. D. K., Nguyen, V. G., & Hoang, A. T. (2024). Nanocomposite from tannery sludge-derived biochar and Zinc oxide nanoparticles for photocatalytic degradation of Bisphenol A toward dual environmental benefits. *Science of The Total Environment*, *907*, 167896. https://doi.org/10.1016/j.scitotenv.2023.167896

V.Samuthira Pandi, B. R. Senthil Kumar, Anusuya, M., & Annu Dagar. (2023). Synthesis and characterization of ZnO, ZnO doped Ag2O nanoparticles and its photocatalytic activity. *The Scientific Temper*, *14*(03), 827–833. https://doi.org/10.58414/SCIENTIFICTEMPER.2023.14.3.41

Yasmin, S. R., Verma, Y., & Lawrence, R. (2021). Biowaste-derived Nanoparticles and Their Preparation: A Review. *The Scientific Temper*, *12*(1 & 2). https://doi.org/10.58414/SCIENTIFICTEMPER.2021.12.1.02

Zhang, X., Cheng, R., Deng, Y., Liu, Z., Liu, X., Liu, Z., Sun, B., Liao, G., & Shi, T. (2024). Tailoring performance of perovskite-based tunneling photodetector for portable monitoring of ultraviolet radiation risk. *Nano Energy*, *122*, 109282. https://doi.org/10.1016/j.nanoen.2024.109282